ChemComm

Chemical Communications

www.rsc.org/chemcomm

Number 6 | 14 February 2008 | Pages 637–784

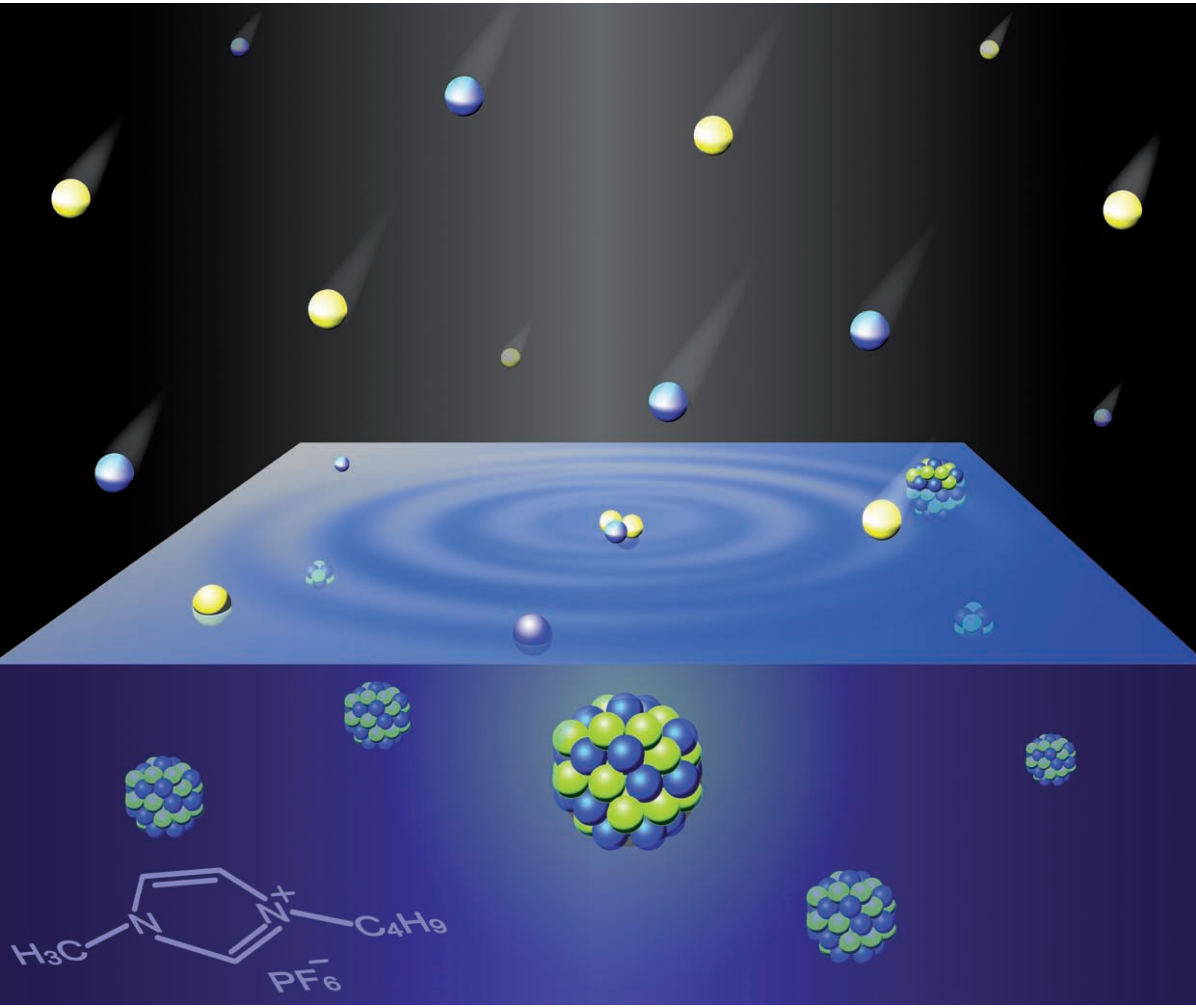

ISSN 1359-7345

RSC Publishing

COMMUNICATION
Tsukasa Torimoto *et al.*
Single-step synthesis of gold–silver alloy nanoparticles in ionic liquids by a sputter deposition technique

Single-step synthesis of gold–silver alloy nanoparticles in ionic liquids by a sputter deposition technique†

Ken-ichi Okazaki,[a] Tomonori Kiyama,[a] Kaori Hirahara,[b] Nobuo Tanaka,[b] Susumu Kuwabata[cd] and Tsukasa Torimoto*[ad]

Received (in Cambridge, UK) 25th September 2007, Accepted 26th November 2007
First published as an Advance Article on the web 4th December 2007
DOI: 10.1039/b714761a

The simultaneous sputter deposition of gold and silver onto ionic liquids formed bimetallic alloy nanoparticles, which exhibited composition-sensitive surface plasmon resonance, the peak wavelength being red-shifted with an increase in the surface area of the gold foil targets sputtered.

Alloy nanoparticles have been attractive materials for applications such as biosensors,[1,2] catalysts[3,4] and optoelectronic devices,[5–7] because they exhibit unique physicochemical properties distinct from those of pure monometallic nanoparticles, being dependent on the size, shape, and composition of particles. So far, several types of bimetallic nanoparticle have been synthesized.[8–11] Especially, the combinations of gold (Au) and silver (Ag) are interesting to investigate for their composition-sensitive optical properties, because monometallic nanoparticles of Au have an intense surface-plasmon absorption peak in the visible region at a wavelength different from that of Ag nanoparticles and because complete miscibility of Au and Ag can be obtained at any composition in both bulk materials and nanoparticles.[12–14] In most cases, Au–Ag nanoparticles have been prepared in solution phase. For example, simultaneous reduction of the corresponding metal ions or metal complexes resulted in the formation of alloy nanoparticles. Mixtures of monometallic Au and Ag nanoparticles enabled the conversion to the alloy by laser irradiation[11,15] or heat treatment in solution.[16]

Ionic liquids (ILs) have been intensively investigated because of their characteristic physicochemical properties, such as high thermal stability, high ionic conductivity and ability to dissolve many kinds of substances. For example, ILs could provide a suitable medium for the preparation and stabilization of various kinds of metal nanoparticles having a narrow size distribution.[17–19] Furthermore, owing to their extremely low vapor pressure,[20] ILs can be treated under high vacuum conditions for XPS[21] and SEM[22] measurements, the fabrication of extremely flat metal mirrors,[23] or the preparation of pure metal nanoparticles.[24] Recently, we have reported an extremely clean method to synthesize Au nanoparticles in ionic liquids (ILs) using a sputter deposition technique without any additional stabilizing agents.[25] It is well known that in sputter deposition under vacuum, the bombardment of a metal target, such as Au foil, with energetic gaseous ions causes the physical ejection of surface atoms and/or small metal clusters. Sputtered Au species were injected into ILs without remarkable gas-phase collisions in the space between the target and IL solution, resulting in the coalescence with each other to form a dispersion of larger Au nanoparticles with diameters of several nanometres. If the sputter deposition of different kinds of pure metals is simultaneously performed onto ILs, their composites on a nanometre scale can be prepared in the solution phase, but this has not been attempted. Here we report an extremely facile single-step strategy to synthesize Au–Ag alloy nanoparticles through the simultaneous sputter deposition of Au and Ag onto ILs.

Ionic liquid 1-butyl-3-methylimidazolium hexafluorophosphate (BMI-PF6) was purchased from Kanto Chemical Co., Inc. and dried for 3 h at 378 K under vacuum before use. A 0.60 cm^3 aliquot of BMI-PF6 was spread on a glass plate (10 cm^2) that was horizontally set in a sputter coater (JEOL, JFC-1300). It was located at a distance of 35 mm from metal targets (diameter: 5 cm) which were composed of radially-arranged Au (99.99% in purity) and Ag (99.99%) foils (Fig. 1a). Each domain had a fan shape with central angle of 30, or 90°, except for the cases of the deposition of pure Au or Ag. The area fraction of gold foils on targets, f_{Au}, was defined as $f_{\mathrm{Au}} = A_{\mathrm{Au}}/(A_{\mathrm{Au}} + A_{\mathrm{Ag}})$, where A_{Au} and A_{Ag} were total

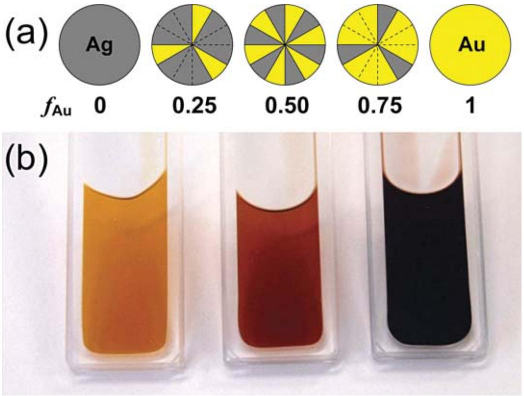

Fig. 1 (a) Schematic illustrations of Au–Ag foil binary targets having various f_{Au}. (b) Photographs of BMI-PF6 obtained after the sputter deposition of Ag (f_{Au} = 0, left), Au–Ag (f_{Au} = 0.50, center) and Au (f_{Au} = 1, right) nanoparticles.

---

[a] *Department of Crystalline Materials Science, Graduate School of Engineering, Nagoya University, Chikusa-ku, Nagoya 464-8603, Japan. E-mail: torimoto@apchem.nagoya-u.ac.jp; Fax: +81-52-789-5299; Tel: +81-52-789-4614*
[b] *EcoTopia Science Institute, Nagoya University, Chikusa-ku, Nagoya 464-8603, Japan*
[c] *Graduate School of Engineering, Osaka University, Suita, Osaka 565-0871, Japan*
[d] *Japan Science & Technology Agency, CREST, Kawaguchi, Saitama 332-0012, Japan*

† Electronic supplementary information (ESI) available: Absorption spectra of mixtures of pure Au and pure Ag nanoparticle solutions. See DOI: 10.1039/b714761a

surface areas of gold and silver foils, respectively. Simultaneous sputter deposition of Au and Ag onto the IL was carried out for 300 s with a current of 40 mA under an argon pressure of *ca.* 20 Pa at room temperature. The structure and size distribution of the nanoparticles were examined using a JEOL JEM-2010 transmission electron microscope (TEM) operated at a 120 kV acceleration voltage. TEM samples were prepared by dropping the IL solution onto a copper TEM grid with amorphous carbon overlayers, followed by the removal of excess amounts of solution with filter paper.

The sputter deposition of pure Ag (f_{Au} = 0) onto BMI-PF6 turned the solution to yellow from colorless (Fig. 1b). In contrast, with an increase in f_{Au}, the solution was a more reddish color and finally became dark red at f_{Au} = 1.0. Fig. 2 shows normalized absorption spectra of BMI-PF6 with the simultaneous sputter deposition of Au and Ag. The spectra were red-shifted with an increase in f_{Au}. In each case, the spectrum exhibited a single peak or shoulder assigned to the surface plasmon resonance (SPR) band of the metal particles. The sputter deposition with f_{Au} of 1.0 and 0, that is, pure Au and pure Ag targets, gave the spectra having peaks at 504 and 404 nm, which were in good agreement with those of the SPR bands reported for Au and Ag nanoparticles,[5,12,13] respectively. Furthermore, the peak SPR wavelength, λ_{SPR}, increased almost linearly with f_{Au}, as shown in the inset of Fig. 2. On the other hand, the absorption spectra of mixtures of pure Au and pure Ag nanoparticle solutions gave two SPR peaks at 504 and 404 nm owing to the superimposition of spectra of corresponding pure metal particles, regardless of the volume ratio of pure Au to pure Ag solutions in mixing (Fig. S1†), as already reported in a previous paper.[11] It is well-known that spherical Au–Ag alloy nanoparticles exhibit a clear single SPR band and that a linear relationship is observed between the mole fraction of Au atoms in alloy particles and λ_{SPR}. Therefore the results in Fig. 2 indicated that the simultaneous injection of sputtered species of Au and Ag into an IL caused a coalescence with each other in the solution, resulting in the formation of alloy nanoparticles of Au–Ag having a single SPR peak, in which the content of Au atoms was proportional to f_{Au}. It is worth mentioning that Au–Ag nanoparticles formed in the IL exhibited a broad SPR band, except for pure Ag particles with f_{Au} = 0. It is well-known that the SPR peak becomes indistinct for pure Au and Au–Ag alloy nanoparticles having the size of a few nanometres.[26] If this situation could be applicable to Au–Ag alloy nanoparticles formed in an IL, the sputter deposition might produce nanoparticles with very small size. This interpretation is supported by TEM observations.

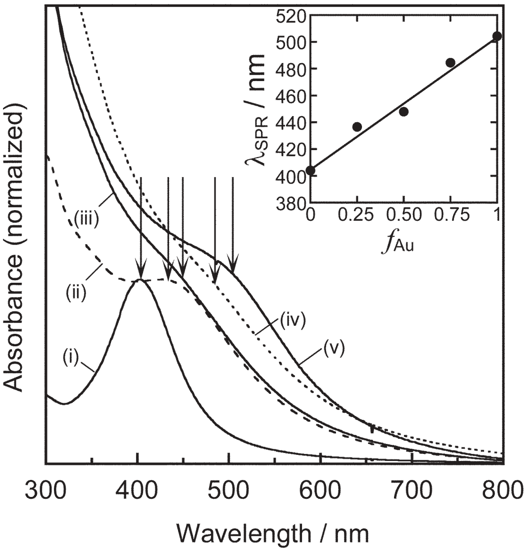

Fig. 2 Normalized absorption spectra of BMI-PF6 after the simultaneous sputter deposition of Au and Ag with f_{Au} = 0 (i), 0.25 (ii), 0.50 (iii), 0.75 (iv) and 1.0 (v). The arrows show the surface plasmon resonance band peak. (Inset) The dependence of the peak wavelength of the SPR band (λ_{SPR}) on f_{Au}.

Fig. 3 shows typical TEM images of pure Ag (f_{Au} = 0), pure Au (f_{Au} = 1.0), and Au–Ag alloy nanoparticles (f_{Au} = 0.50) in BMI-PF6. In each case, the sputter deposition produced spherical particles highly-dispersed in the IL. Individual nanoparticles were single crystals, having clear lattice fringes without exhibiting lattice mismatch or lattice defects inside the particles, even in the case of f_{Au} = 0.50. The prepared nanoparticles gave almost the same interplanar spacings for lattice fringes within experimental errors, *ca.* 0.235 nm, regardless of the f_{Au} values, which were assignable to (111) planes of the face-centered cubic structures of the corresponding bulk metals. These were reasonable because gold and silver have very similar lattice constants of 0.4078 and 0.4086 nm.[27,28] Elemental analyses of nanoparticles with energy dispersive X-ray spectroscopy (EDX) performed at the same time as the TEM observations revealed that nanoparticles obtained with f_{Au} = 0.50 were composed of Au and Ag atoms with the molar ratio of Au : Ag = 0.52 : 0.48. On the other hand, the mole fraction of Au atoms in the alloy particles could be estimated to 0.56, by fitting the λ_{SPR} obtained at f_{Au} = 0.50 in Fig. 2 to the previously reported relationship between λ_{SPR} and the mole fraction of Au atoms in alloy particles.[8] Although the λ_{SPR} peaks were indistinct due to the size of the alloy particles being a few nanometres, a relatively good agreement was observed between the result determined from EDX and that estimated from absorption spectra. This result suggested that the fluctuation in alloy composition of individual alloy particles was small enough to be neglected.

The size distributions of the nanoparticles were determined by measuring the sizes of individual particles in TEM images (more than 100 particles). The pure Au nanoparticles (f_{Au} = 1.0) in BMI-PF6 had an average diameter (d_{av}) of 2.6 nm with a standard deviation (σ) of 0.3 nm. The decrease in f_{Au} brought about the enlargement of the particle size: d_{av} (σ) was 3.1 (0.6) and 6.0 nm (1.5 nm) with 0.5 and 0, respectively. It has been reported in our previous paper[25] that the size of Au nanoparticles sputter-deposited in ILs varies with the kind of IL used, probably because of the prevention of coalescence between particles by the strong adsorption of IL species on the surface and by electrostatic repulsion between the resulting particles. Since the adsorption strength of ILs on the particle surface was expected to be dependent on the kind of metal nanoparticles as well as the IL used, it was suggested that the size of nanoparticles was determined by the difference in the adsorption strength of BMI-PF6 on metal sites of the surface: the relatively strong adsorption of IL could suppress the growth and/or coalescence of particles.

In conclusion, the simultaneous sputter deposition of pure metals on ILs was demonstrated to be an extremely facile synthetic

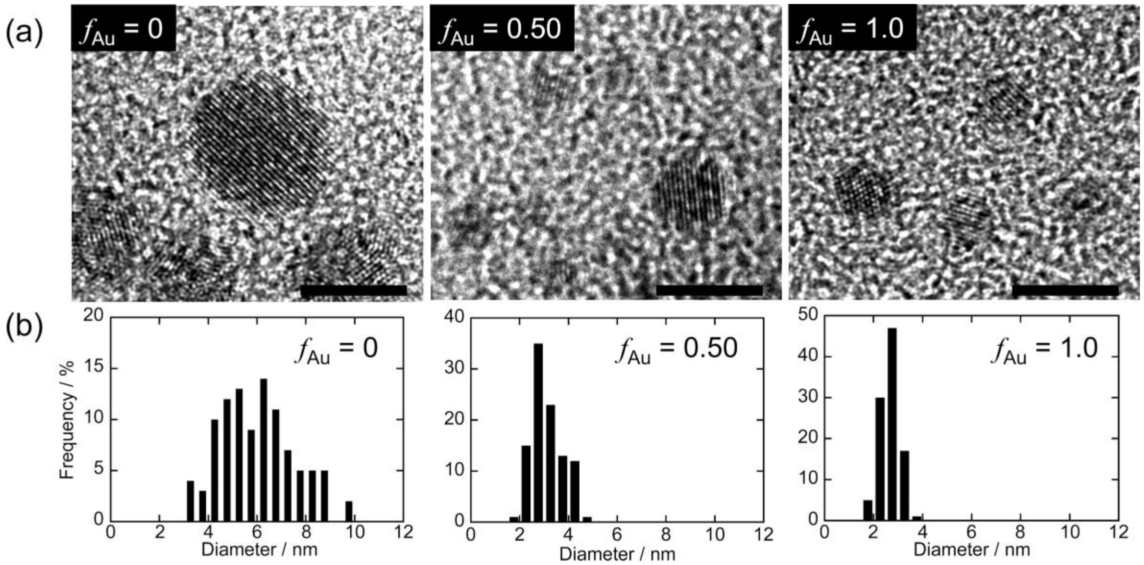

Fig. 3 TEM images (a) and size distributions (b) of Au–Ag alloy nanoparticles obtained by the sputter deposition onto BMI-PF6 with f_{Au} = 0, 0.50 and 1.0. The bars in the pictures represent a length of 5 nm.

method to prepare bimetallic alloy nanoparticles. The chemical composition and optical properties of the alloy nanoparticles were easily controlled just by varying the area ratio of the individual pure metal foils in the sputtering targets. Although the preparation of only Au–Ag alloy nanoparticles is described in this paper, the present technique enables the formation of novel alloy nanoparticles in solutions, which have never been produced by conventional solution strategies, such as the simultaneous chemical reduction of several metal salts, where metal ions having more positive redox potential tend to be preferentially reduced. Furthermore, the simultaneous sputter deposition of different kinds of pure materials can be applied to prepare alloy nanoparticles containing three or more elements, the physicochemical properties being tunable for desired purposes, such as catalysts for fuel cells. Study along this line is currently in progress.

This research was partially supported by a Grant-in-Aid for Exploratory Research (No. 19655075) from the Japan Society for the Promotion of Science and by a Grant-in-Aid for Scientific Research on Priority Area (470) "Strong Photons-Molecules Coupling Fields" and on Priority Area (452) "Science of Ionic Liquids" from the Ministry of Education, Culture, Sports, Science and Technology (MEXT) of Japan. K. O. thanks Grant-in-Aid for Young Scientists (B) (No. 18750180) from MEXT.

Notes and references

1 K. S. Lee and M. A. El-Sayed, *J. Phys. Chem. B*, 2006, **110**, 19220–19225.
2 L. Y. Wang, X. J. Shi, N. N. Kariuki, M. Schadt, G. R. Wang, Q. Rendeng, J. Choi, J. Luo, S. Lu and C. J. Zhong, *J. Am. Chem. Soc.*, 2007, **129**, 2161–2170.
3 G. Schmid, H. West, H. Mehles and A. Lehnert, *Inorg. Chem.*, 1997, **36**, 891–895.
4 M. S. Nashner, A. I. Frenkel, D. L. Adler, J. R. Shapley and R. G. Nuzzo, *J. Am. Chem. Soc.*, 1997, **119**, 7760–7771.
5 P. Mulvaney, *Langmuir*, 1996, **12**, 788–800.
6 M. Valden, X. Lai and D. W. Goodman, *Science*, 1998, **281**, 1647–1650.
7 L. M. Liz-Marzan, *Langmuir*, 2006, **22**, 32–41.
8 S. Link, Z. L. Wang and M. A. El-Sayed, *J. Phys. Chem. B*, 1999, **103**, 3529–3533.
9 L. Rivas, S. Sanchez-Cortes, J. V. Garcia-Ramos and G. Morcillo, *Langmuir*, 2000, **16**, 9722–9728.
10 M. Yamamoto and M. Nakamoto, *Chem. Lett.*, 2003, **32**, 452–453.
11 Z. Q. Peng, B. Spliethoff, B. Tesche, T. Walther and K. Kleinermanns, *J. Phys. Chem. B*, 2006, **110**, 2549–2554.
12 G. C. Papavassiliou, *J. Phys. F: Met. Phys.*, 1976, **6**, L103–L105.
13 P. Mulvaney, M. Giersig and A. Henglein, *J. Phys. Chem.*, 1993, **97**, 7061–7064.
14 N. N. Kariuki, J. Luo, M. M. Maye, S. A. Hassan, T. Menard, H. R. Naslund, Y. H. Lin, C. M. Wang, M. H. Engelhard and C. J. Zhong, *Langmuir*, 2004, **20**, 11240–11246.
15 F. Hajiesmaeilbaigi and A. Motamedi, *Laser Phys. Lett.*, 2007, **4**, 133–137.
16 A. B. Smetana, K. J. Klabunde, C. M. Sorensen, A. A. Ponce and B. Mwale, *J. Phys. Chem. B*, 2006, **110**, 2155–2158.
17 E. T. Silveira, A. P. Umpierre, L. M. Rossi, G. Machado, J. Morais, G. V. Soares, I. L. R. Baumvol, S. R. Teixeira, P. F. P. Fichtner and J. Dupont, *Chem.–Eur. J.*, 2004, **10**, 3734–3740.
18 Y. Wang and H. Yang, *J. Am. Chem. Soc.*, 2005, **127**, 5316–5317.
19 L. Yu, H. Sun, J. He, D. Wang, X. Jin, M. Hu and G. Z. Chen, *Electrochem. Commun.*, 2007, **9**, 1374–1381.
20 M. J. Earle, J. Esperanca, M. A. Gilea, J. N. C. Lopes, L. P. N. Rebelo, J. W. Magee, K. R. Seddon and J. A. Widegren, *Nature*, 2006, **439**, 831–834.
21 E. F. Smith, I. J. Villar Garcia, D. Briggs and P. Licence, *Chem. Commun.*, 2005, 5633–5635.
22 S. Kuwabata, A. Kongkanand, D. Oyamatsu and T. Torimoto, *Chem. Lett.*, 2006, **35**, 600–601.
23 E. F. Borra, O. Seddiki, R. Angel, D. Eisenstein, P. Hickson, K. R. Seddon and S. P. Worden, *Nature*, 2007, **447**, 979–981.
24 S. A. Meiss, M. Rohnke, L. Kienle, S. Z. El Abedin, F. Endres and J. Janek, *ChemPhysChem*, 2007, **8**, 50–53.
25 T. Torimoto, K. Okazaki, T. Kiyama, K. Hirahara, N. Tanaka and S. Kuwabata, *Appl. Phys. Lett.*, 2006, **89**, 243117.
26 O. M. Wilson, R. W. J. Scott, J. C. Garcia-Martinez and R. M. Crooks, *J. Am. Chem. Soc.*, 2005, **127**, 1015–1024.
27 *Powder Diffraction Data File*, JCPDS-International Center for Diffraction Data, 4–0784.
28 *Powder Diffraction Data File*, JCPDS-International Center for Diffraction Data, 4–0783.